Measurement of Diffusivities of Sulfur Mustard (SM) and Its Analog Oxygen Mustard (OM) in Cured Butyl, Nitrile, and Natural-Rubber Sheets by Weight Gain and FTIR–ATR Methods

SUSANTA BANERJEE,* RAJENDRA P. SEMWAL, and SEEMA AGARWAL

Defence Research & Development Establishment, Jhansi Road, Gwalior - 474002, India

SYNOPSIS

The breakthrough time of butyl, nitrile, and natural-rubber sheets (cured) of different compositions against a potent chemical warfare (CW) agent have been determined using the spot disc test (SDT) method. It was observed that butyl rubber is the best material in comparison to nitrile and natural rubber for protection against sulfur mustard (SM). One of the butyl formulations provides more than 100 h protection against SM. The diffusion coefficient of oxygen mustard (SM analog) for the same formulation (F_8) and one nonblack butyl formulation (F_5) was determined by weight gain as well as by FTIR–ATR methods. Both methods provide consistent results and the diffusion coefficient of oxygen mustard (OM) for butyl rubber is in the order of 10^{-9} cm²/s. The diffusion coefficient of SM for the formulation F_8 and F_5 was also determined from the SDT retardation time. © 1995 John Wiley & Sons, Inc.

INTRODUCTION

Sulfur mustard (SM), chemically known as thiobis-(1,1-dichloroethane), is a well-known vesicant. It is one of the oldest alkylating agents and damages body cells seriously on short-term exposure at very low concentrations. Moreover, it is alleged to have been used in the Iran–Iraq conflict. Of the many chemical warfare (CW) agents known today, SM is notorious for its permeability through varieties of material and, therefore, it is the candidate agent against which protective materials should be tested.

The study of the sorption/diffusion of liquids, gases, and vapors through polymers is of great interest due to their diversified applications as thickners, protective coatings, artificial leathers, packaging materials, membranes, and so forth. The literature[1-8] is replete with the diffusion of industrial solvents through different engineering plastics/elastomers. The diffusion of organic liquids through polymers depends on the nature of the polymer, temperature, concentration of the penetrant, and shape and size of the diffusive molecules.[1] For molecules of low solubility, the polymer matrix is unaffected by the diffusant, so that the diffusion is expected to follow Fick's laws.[9] The rate of change of concentration at any point can be found by Fick's second law:

$$dc/dt = Dd^2c/dx^2 \qquad (1)$$

The above equation has several solutions, depending on the boundary and, consequently, experimental conditions. The most commonly used method of determining D is the sorption–desorption (weight gain) method.[10] The sorption–desorption method consists of the study of kinetics of liquid sorption by a polymer sample under isobaric–isothermal conditions. If the liquid-sorbing sample is a plate of thickness L, then, under the boundary conditions $0 < x < L$ and $0 < C < C_{equiv.}$, the Fick's second law solved as follows:

$$M_t/M_\infty = 4/L(Dt/\pi)^{1/2} \qquad (2)$$

M_t = amount of sorbate or desorbate by the moment of time t, and M_∞ = equilibrium amount of the sorbate. The diffusion is claimed to follow the Fickian kinetics when the plot of M_t/M_∞ vs. $f(t^{1/2})$ is an L-shaped curve with its initial rectilinear part in the region of $M_t/M_\infty < 0.6$ and D may be calculated from the slope of the rectilinear part of the curve.[11]

Fourier-transform infrared spectroscopy (FTIR), with the attenuated total reflactance (ATR) sampling method, provides another method for measuring diffusivities of slowly diffusing, IR active species.[12–14] The FTIR–ATR method provides a few advantages over sorption–desorption/gravimetric methods for determining diffusivities. In the case of a mixture of diffusants, simultaneous measurement of diffusivities is possible provided that each diffusant has a well-separated IR peak. Changes, if any, of the IR spectrum of the polymer can also be obtained, which provide information about chemical reactions/physical interactions (e.g., hydrogen bonding) that may occur between the polymer and the diffusant.

The aim of the present investigation was as follows:

(i) Study of the diffusion of oxygen mustard (OM) and sulfur mustard (SM) through butyl rubber.

(ii) Development of a suitable face mask material for protection against CW agents based on the results.

(iii) A new methodology for obtaining diffusion coefficients using FTIR–ATR.

EXPERIMENTAL

Materials

Polymer sheets of butyl, nitrile, and natural rubber of different dimensions were molded using a mold of different dimensions on a hydraulic press. The mixing of the rubbers was done using a 30.48 cm laboratory mixing mill. The composition of the different formulations are given in Table I. The cured time of the different formulations at 170°C were determined using a Monsanto R-100 Rheometer. From the rheographs, the scorch time and optimum cure time (t_{90}) were determined. The butyl sheets were press-cured at 170°C from 35 to 40 min, nitrile sheets were press-cured at 170°C for 9 min, and natural rubber was press-cured at 170°C for 7 min. The mechanical properties of the aged and non-aged sheets are reported in Table II. Exxon butyl-268, nitrile rubber-JSR 230S, and RAMIX-grade natural rubber were used for the preparation of cured sheets. Black HAF-N330 (Philips Carbon, India), zinc oxide (G.R) (S.D., India), MBTS (Bayer, Germany), stearic acid (Stā) (Wilson, India), and sulfur (LR) (Qualigens, India) were used as received.

Oxygen mustard (OM) (E. Merck, Germany) was distilled prior to use. Sulfur mustard (SM) was synthesized by the known method[15] and the GLC purity was 99.9%.

Table I Composition of Different Formulations (in phr) and SM BTT by SD Test[a]

Formulations	Butyl Rubber	Nitrile Rubber	Natural Rubber	Black HAF-N330	Oil	ZnO	Sta	MBTS	Sulfur	Thickness (mm)	BTT (hr)
F_1	100	—	—	30	20[b]	5	2	1	2	1.8	48
F_2	100	—	—	40	20[b]	5	2	1	2	1.8	52
F_3	100	—	—	50	20[b]	5	2	1	2	1.8	61
F_4	100	—	—	60	20[b]	5	2	1	2	1.8	46
F_5	100	—	—	—	—	5	2	1	2	1.8	24
										0.5	5
F_6	—	100	—	50	10[c]	5	2	1	2	1.8	28
F_7	—	—	100	50	10[d]	5	2	1	2	1.8	4
F_8	100	—	—	50	10[b]	5	2	1	2	1.8	> 100
										0.5	16
F_9	100	—	—	50	5[b]	5	2	1	2	1.8	80
										0.5	12

[a] Average of three consistant readings.
[b] Paraffinic.
[c] Aromatic.
[d] Naphthanic.

Table II   Mechanical Properties of the Different Cured Sheets Before and After Aging at 100 ± 2°C for 10 Days

Sheet Code (Formulation)	300% Modulus[a] (kg/cm^2)	Tensile Strength[a] (kg/cm^2)		RTS[b] (%)	% Elongation[a] at Break		Hardness[c] Shore "A"	
		Nonaged	Aged		Nonaged	Aged	Nonaged	Aged
F_1	13.2	106.0	112.0	105.6	850	758	38	44
F_2	14.0	116.8	121.7	104.2	838	759	39	46
F_3	14.6	128.5	136.7	106.4	832	748	40	46
F_4	20.3	129.6	133.2	102.7	820	695	51	56
F_5	—	19.4	—	—	320	—	32	—
F_6	39.9	130.7	117.7	85.4	600	415	60	71
F_7	38.2	132.8	94.7	71.3	650	350	57	72
F_8	39.7	140.9	149.9	106.4	750	685	50	56
F_9	38.2	135.8	144.2	106.1	730	618	53	57

[a] ASTM D 412.
[b] RTS: retention of tensile strength.
[c] ASTM D2240.

Procedure

Spot Disc (SD) Test (Breakthrough Time, BTT Test)

The permeation resistance of the sheets were evaluated by the known SD test method[16] as follows: A test specimen (6 × 6 cm^2) was sealed on a Congo Red paper (5 × 5 cm^2) having tiny drops of the SD (2,4-dichlorophenyl benzoyl chloride) reagent. SM, 100 µL, was deposited on a Whattman No. 1 filter paper piece and an inverted Petri dish was kept and sealed on top of the test specimen for preventing the SM from evaporating. The whole assembly was thermostated at 37 ± 1°C. The underside of the detector paper was observed using a 45° mirror located under the glass plate for the appearance of the blue spots. SM penetrating the test specimen gives rise to the occurrence of blue spots caused by hydrogen chloride resulting from the reaction between chloroimide and SM. BTT was taken as the time for the appearance of blue spots.

Weight Gain Experiment

Sheets, 2 × 4 cm^2, of F_5 and F_8 formulations (thickness 0.15 mm) were cut into pieces and dried in a vacuum oven at 100°C for 5 h to remove surface-absorbed moisture. The pieces were dipped into an adequate amount of OM and the sample weights before and after exposure of different time periods were determined by a Mettler analytical balance having a sensitivity of 10^{-6} g. The temperature was thermostated at 25 ± 1°C.

FTIR–ATR Measurements

A Perkin-Elmer 1720 × FTIR spectrometer equipped with a DTGS detector and a flat-plate ATR sampling accessory was used to obtain the IR spectra. A KRS-5 parallelogram crystal with an angle of incidence of 45° was used. All ATR spectra were collected at a 4 cm^{-1} resolution, and 10 scans were accumulated for each sample. Computer substractions between spectra were performed with the use of the band at 1120 cm^{-1} as a reference which was attributed to a C—O—C stretching vibration associated with the OM and does not overlap with other bands. For the FTIR–ATR experiment, one side of a 5 × 5 cm^2 butyl rubber sheet of 0.15 mm thickness was exposed to 100 µL OM and the sheets were allowed to absorb OM in a closed chamber and then cut into 1 × 5 cm^2 sheets and kept in the ATR sampling accessory. The unexposed side
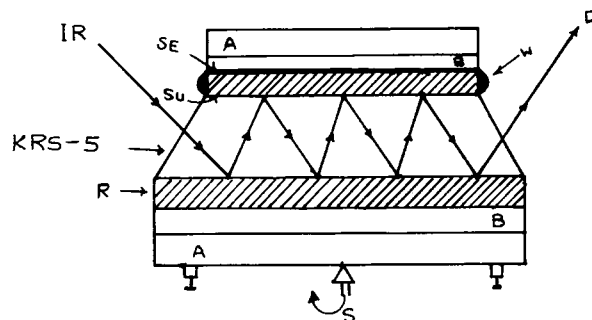
Sketch of the ATR sampling. SE = sample exposed surface; R = reference.

Table III Sorption and Diffusion Data by Weight Gain Method

Dipping Time (min)		$t^{1/2}$		Weight Gain $\times 10^3$		M_t/M_∞		% Weight Gain/Sorption Coefficient (cm³/cm³ atm)	
F_5	F_8	F_5	F_8	F_5	F_8	F_5	F_8	F_5	F_8
5	30	2.23	5.48	0.730	1.011	0.22	0.30		
10	60	3.16	7.74	1.062	1.516	0.32	0.45		
15	90	3.87	9.48	1.328	1.891	0.40	0.50		
20	120	4.47	10.95	1.494	2.089	0.45	0.62		
25	150	5.00	12.24	1.660	2.291	0.50	0.68		
30	180	5.48	13.41	1.759	2.493	0.53	0.74		
35	210	5.91	14.49	1.958	2.696	0.59	0.80		
40	240	6.32	15.49	2.124	2.898	0.64	0.86		
45	270	6.70	16.43	2.224	3.100	0.67	0.92		
50	300	7.07	17.32	2.390	3.235	0.72	0.96		
55	330	7.41	18.16	2.490	3.268	0.75	0.97		
60	360	7.74	18.97	2.622	3.302	0.79	0.98		
70	390	8.36	19.74	2.788	3.312	0.84	0.98		
80	420	8.94	20.49	2.988	3.336	0.90	0.99		
100	450	10.00	21.21	3.154	3.360	0.95	0.99		
120	480	10.95	21.90	3.220	3.370	0.97	1.00	—	$1.73/2.30 \times 10^{-2}$
140	—	11.83	—	3.286	—	0.99	—		
170	—	13.03	—	3.320	—	1.00	—	$2.45/2.27 \times 10^{-2}$	—

[a] Initial weight of F_5 = 0.135605 g; volume = 2 × 4 × 0.015 cm³ = 0.120 cm³; density = 1.130 g/cm³.
Initial weight of F_8 = 0.194400 g; volume = 2 × 4 × 0.015 cm³ = 0.120 cm³; density = 1.162 g/cm³.
Density of DM at 25°C = 1.217 g/cm³.
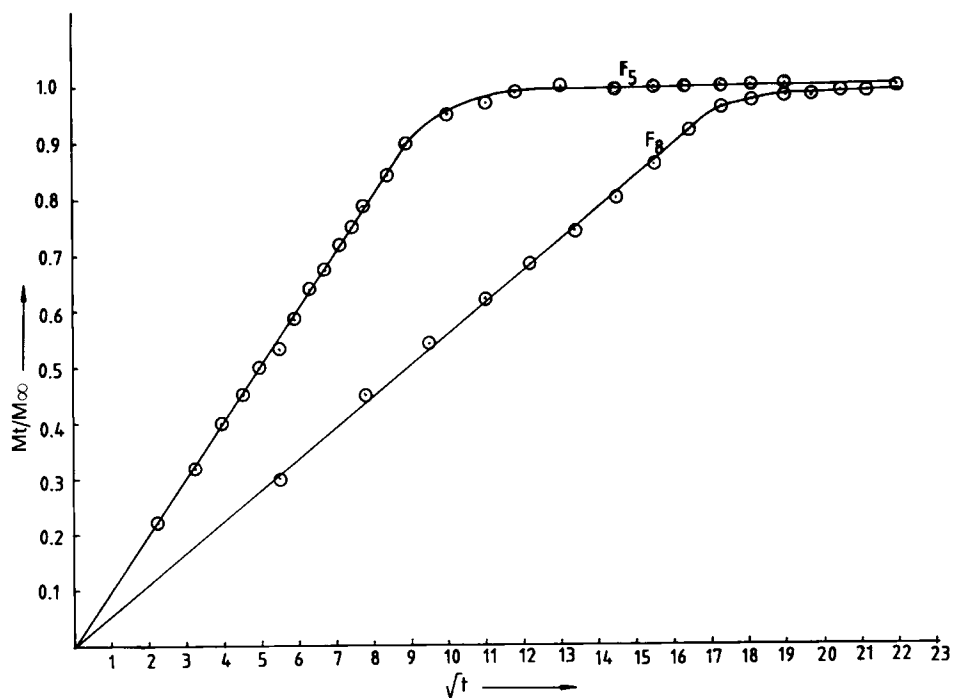
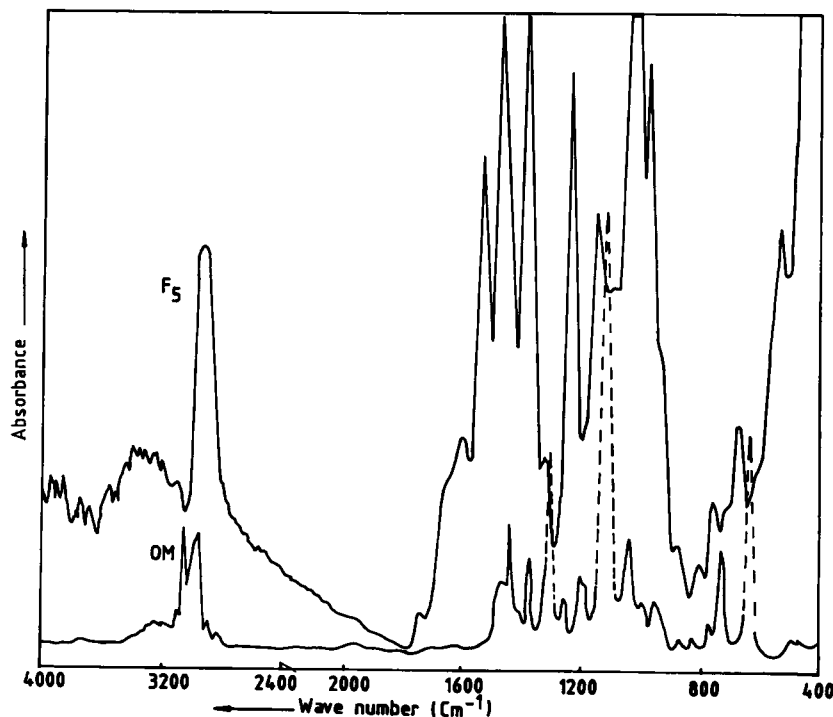**Figure 1** Plot of M_t/M_∞ vs. $t^{1/2}$.

Figure 2   IR spectra of cured nonblack butyl sheet (F_5) and OM.
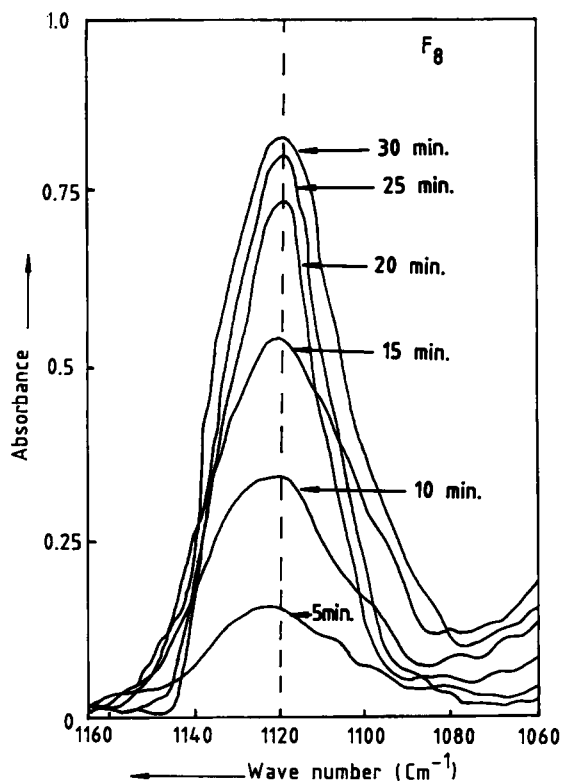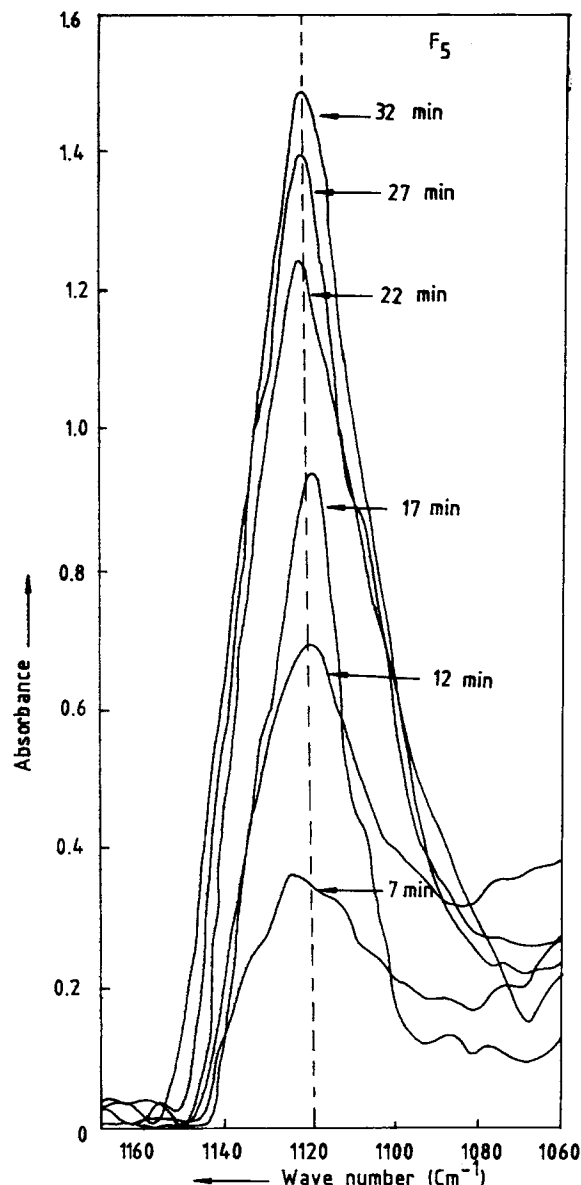

Figure 3   IR spectra of diffused OM through F_8 at different intervals of time.

faced the KRS-5 crystal. The cross section of the ATR sampling is shown in the following sketch.

RESULTS AND DISCUSSION

From the data presented in Table I, it is clear that butyl rubber provides maximum protection toward SM. In the case of natural rubber (NR), the low BTT value can be explained due to its highly amorphous structure, chain flexibility, and comparatively weak interchain interaction facilitating the permeation of penetrant molecules. Nitrile rubber (NBR) provides more protection time than does NR. It has already been reported in the literature[11] that substituents like —Cl, —C_6H_5, —OH, and —C≡N in the polymer chain can greatly change the interchain interaction and, as a result, decrease the free activation energy of the diffusion and permeability. Hence, the greater BTT of NBR can be understood. The best protection by butyl rubber (IIR) toward SM is due to its highly symmetric structure which increases the macromolecular packing density and, therefore, is not conducive to high values of permeability. As the loading of the reinforcing black filler increases (F_1–F_4) from 30 to 50 phr, the permeation time of SM increases accordingly and it
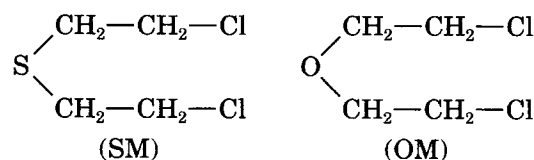
Figure 4 IR spectra of diffused OM through F_5 at different intervals of time.

decreases again when the loading of black is 60 phr, keeping the same amount of oil in all the formulations (20 phr). The same trend is observed in the mechanical properties of the formulations F_1–F_4 (Table II). To study the effect of oil on the permeation, three different formulations, F_3, F_8, and F_9, having an oil content of 20, 10, and 5 phr with the same amount of black (50 phr), were prepared. Formulation F_8, where the oil content is 10 phr, provided the highest SM BTT as well as mechanical properties. Formulation F_9 provided inferior results to those of F_8, which can be attributed to the poor dispersion of black in the rubber matrix. The me-

chanical properties of the same formulations (Table II) can also be explained similarly. Hence, formulation F_8 turns out to be the best. In general, all the butyl formulations after aging at 100°C for 10 days provide better tensile properties than do the unaged one. This is due to the increase of crosslink density after prolonged aging and to the absence of any oxidizable linkages in the polymer backbone in comparison to nitrile and natural rubber.

Due to handling difficulties of SM, OM was used as a model compound for the diffusion experiment. The chemical structure of the above two compounds are given below:

$$S \Big\langle \begin{array}{l} CH_2-CH_2-Cl \\ CH_2-CH_2-Cl \end{array} \qquad O \Big\langle \begin{array}{l} CH_2-CH_2-Cl \\ CH_2-CH_2-Cl \end{array}$$
(SM) (OM)

The diffusion coefficients of OM through two different butyl formulations F_5 (nonblack) and F_8 were determined at 25°C by weight gain and FTIR–ATR methods. The weight gain by the sheets of F_5 and F_8 formulations after different intervals of time are presented in Table III. It is observed that the F_8 formulation takes the maximum time to reach equilibrium sorption, but the weight gained after reaching equilibrium for both formulations are comparable. From this observation, it can be said that the diffusion of sorbate molecules through F_5 is faster than it is through F_8.

To confirm whether the sorption mechanism follows the Fickian mode or not, the dynamic sorption results for the short time ($M_t/M_\infty < 0.6$) were fitted to the empirical expression[17]

$$M_t/M_\infty = Kt^n \tag{3}$$

where M_t and M_∞ are same as defined earlier, and K is a constant characteristic of the polymer–solvent system. For a polymer with slab geometry, a value of $n = 0.5$ indicates the Fickian mode of transport, while $n = 1$ indicates case II (relaxation-controlled) transport; values of n between these limits define anomalous transport.[18] The n and K values were calculated from the plot of Ln M_t/M_∞ vs. Ln t. The values of n are 0.500 and 0.489 for F_5 and F_8, respectively. The lower K value for F_8 ($K = 0.06$) than for F_5 ($K = 0.100$) indicates less solvent–substrate interaction in the black-loaded butyl formulation, and as a result, the diffusion coefficient of F_8 is expected to be lower than that of F_5.
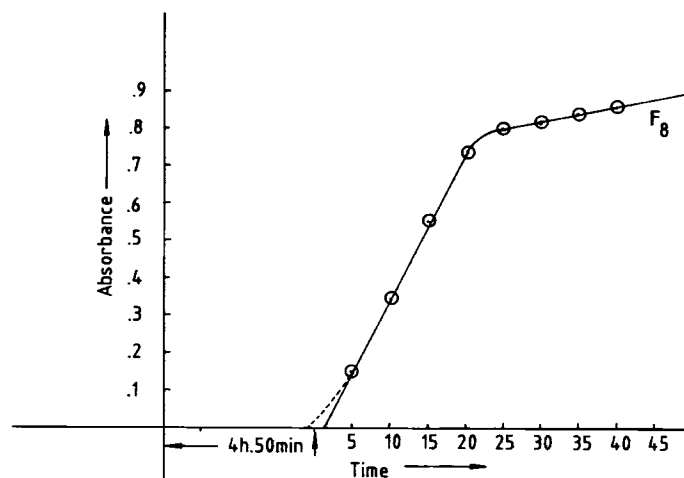
Figure 5   Plot of absorbance vs. time for F_8.

The diffusion coefficient of OM through F_5 and F_8 sheets was calculated using eq. (2) from the plot of M_t/M_∞ vs. $t^{1/2}$ shown in Figure 1. The diffusion coefficient of F_5 is 7.36×10^{-9} cm^2/s and that of F_8 is 2.2×10^{-9} cm^2/s. The low value of the diffusion coefficient of F_8 may be due to less solvent–sorbate interaction between OM and black-loaded rubber. The diffusion coefficients of nitrile (F_6) and natural (F_7) rubber samples were not obtained from the weight gain experiment because of their nonlinear sorption-uptake responses with the square root of time.

FTIR–ATR spectra of the unexposed F_5 sheet and OM is shown in Figure 2. As seen in the figure, 1120 cm^{-1} is a characteristic absorbance band due to the C—O—C stretching vibration of OM. The exposed sheets of F_5 and F_8 were kept in the ATR accessory and monitored at different intervals of time to determine the correct retardation time (θ) (from exposure time to detection time). The increment of OM to the permeation side of F_5 and F_8 is shown in Figures 3 and 4, respectively. The diffusion coefficient was calculated using the following equation (one of the solutions of Fick's second law, when boundary conditions are $X = 0$ and $X = L$ [L = thickness of sheet, θ = retardation time]):

$$D = L^2/6\theta \qquad (4)$$

The diffusion coefficient values from FTIR–ATR were calculated from the plot of relative absorbance vs. time (Figs. 5 and 6) and the results are comparable with the values obtained from the weight gain method (Table IV). In the case of F_5, the value of the diffusion coefficient by FTIR–ATR is higher than is the value obtained by the weight gain

method. This is because of the translucent nature of F_5, which allows the penetration of IR radiation (at 1120 cm^{-1}) and provides less retardation time.

To understand the chemical/physicochemical interaction between OM and the butyl formulation (F_5), the FTIR–ATR spectra of the exposed and unexposed samples were compared. It was found that both the spectra match completely. Hence, there is no interaction between OM and F_5. The same observation was also found in the case of SM and F_5.

The diffusion coefficient of SM through F_5 and F_8 was calculated from spot disc (SD) test data at 25°C assuming Fickian behavior. To calculate the diffusion coefficient, the SD permeation time was considered the same as the retardation time in FTIR–ATR method. The low value of the diffusion coefficient of SM (Table IV) may be assumed due to the presence of the bulky S atom in SM in comparison to the O atom in OM and less plasticization
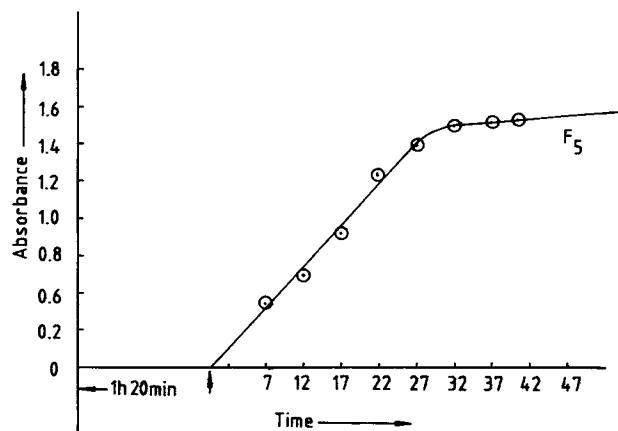

Figure 6   Plot of absorbance vs. time for F_5.

Table IV   Diffusion Coefficient (D) (cm^2/s) Data for OM and SM

| Formulation | Spot Disc (SD) Test[a] | | | Weight Gain (of OM) | | FTIR–ATR | |
	Thickness (cm)	BTT (min)	D of SM	D	P[b]	Retardation Time (min)	D of OM
F_5	0.015	150	4.16×10^{-9}	7.36×10^{-9}	1.67×10^{-10}	80	7.81×10^{-9}
F_8	0.015	400	1.56×10^{-9}	2.20×10^{-9}	5.06×10^{-11}	292	2.14×10^{-9}
F_6	0.053	18	4.33×10^{-7}	—	—	13	6.00×10^{-7}
F_7	0.053	140	5.57×10^{-8}	—	—	110	7.09×10^{-8}

[a] The test was performed at 25°C.
[b] P stands for permeability coefficient (cm^3 cm/cm^2 s atm).

of the butyl formulation caused by SM than by OM, although further investigation is required to understand these phenomena.

The diffusion coefficients of SM and OM for nitrile (F_6) and natural (F_7) rubber formulations were also calculated from SD, BTT, and FTIR–ATR retardation times, respectively. The time-lag plot obtained (absorbance vs. time) from the FTIR–ATR results is not very linear. Therefore, the results presented for F_6 and F_7 in Table IV should be viewed with skepticism.

CONCLUSION

From the above investigation it can be concluded that butyl rubber is the best material for protection against SM. This study also shows that FTIR–ATR is a suitable technique to calculate the retardation time as well as the diffusion coefficient.

REFERENCES

1. M. Saleen, A.-F. A. Asfour, and D. Dee Kee, *J. Appl. Polym. Sci.*, **37**, 617 (1989).
2. R. Forte and J. L. Leblanc, *J. Appl. Polym. Sci.*, **45**, 1473 (1992).
3. P. E. Cassidy, T. M. Aminabhavi, and J. C. Brunson, *Rubb. Chem. Technol.*, **56**, 357 (1983).
4. P. E. Cassidy, T. M. Aminabhavi, and M. C. Thompson, *Rubb. Chem. Technol.*, **59**, 779 (1986).
5. U. S. Aithal, T. M. Aminabhavi, and S. S. Shukla, *Chem. Eng. Data*, **35**, 298 (1990).
6. U. S. Aithal, T. M. Aminabhavi, and P. E. Cassidy, ACS Symp. Ser. 423, American Chemical Society, Washington, DC, 1990, p. 351.
7. B. D. Barr-Howell and N. A. Peppas, *J. Appl. Polym. Sci.*, **31**, 39 (1986).
8. S. B. Harogoppad and T. M. Aminabhavi, *Macromolecules*, **24**, 2598 (1991).
9. T. M. Aminabhavi and R. S. Khinnavar, *Polymer*, **34**, 1006 (1993).
10. R. M. Felder and G. S. Huvard, in *Methods of Experimental Physics*, R. A. Fava, Ed. (Academic Press, New York, 1980), Vol. 16, Part C, p. 315.
11. A. Tager, *Physical Chemistry of Polymers*, 2nd ed. (Mir, Moscow, 1978) Chap. 21.
12. J. R. Xu and C. M. Balik, *Appl. Spectrosc.*, **42**, 1543 (1988).
13. R. P. Semwal, N. B. S. N. Rao, and B. P. Hajela, *Spectrochem. Acta*, **48A**, 1045 (1992).
14. G. T. Fieldson and T. A. Barbari, *Polymer*, **34**, 1146 (1993).
15. H. T. Clarks and D. S. Gasch, *J. Chem. Soc.*, **101**, 1583 (1912).
16. H. F. G. Oudmayer and P. P. M. M. Wittgen, TNO Report PML 1991-82, TNO Prins Maurits Laboratory, Netherlands, November 1991, p. 16.
17. M. N. Franson and N. A. Peppas, *J. Appl. Polym. Sci.*, **28**, 1299 (1983).
18. U. S. Aithal, T. M. Aminabhavi, and P. E. Cassidy, *J. Membr. Sci.*, **50**, 225 (1990).